# In-situ validation of a sizing method for the combined production and distribution of heat for space heating and domestic hot water

# In-situ validation of a sizing method for the combined production and distribution of heat for space heating and domestic hot water

Senne Van Minnebruggen[a]*, Houssam Matbouli[a], Stef Jacobs[a], Ivan Verhaert[a]

[a]*EMIB, Faculty of Applied Engineering – Electromechanics, University of Antwerp, Groenenborgerlaan 171, Antwerp 2020, Belgium*
**Corresponding Author: senne.vanminnebruggen@uantwerpen.be*

ABSTRACT

Collective heating systems are a cost-efficient way to integrate sustainable heat supply in buildings. However, to maximize their potential proper sizing is fundamental. In this respect, various sizing approaches are found to be insufficient according to initial evaluation and feedback from designers. To address this design problem, a novel sizing approach "maximum sum of parts" has been introduced. This research presents a validation methodology, utilizing residential heat meter data to affirm the validity of the sizing approach while addressing the limitations to determine the design peak heat demand from meter readings. It reveals a thermal power-storage characteristic, providing insights into the required combinations to meet the peak heat demand, necessary to evaluate the outcome of the sizing approach. The application of this methodology to six case studies validates the sizing approach. However, under-sizing problems may arise when decentralized storage is taken into account in the sizing approach.

*Keywords:*
Collective heating systems, Design heat load estimation, Combined heat distribution systems, Residential heating systems

# 1 Introduction

Collective heating and cooling systems are part of the solution to shift towards a renewable and climate-neutral energy supply. The potential advantages of implementing collective heating systems are well documented in academic literature [1], [2]. More specific, the integration of collective heating systems offers the scale advantages and/or the required flexibility to increase the amount of intermittent renewable energy sources in the overall energy supply, resulting in the potential to lower CO2-emissions. These advantage not only apply to the level of districts but also to the level of collective residential buildings.

In collective residential buildings, combined heat distribution circuits (CHDC), known as 'Combilus' in Belgium, are considered state-of-the-art. These systems distribute heat for both space heating (SH) and domestic hot water (DHW) using only one supply and one return pipe. Studies comparing the different residential heating systems show that the CHDC has lower distribution heat losses, lower operating costs, and the potential to lower the temperature regime [3], [4]. Moreover, the CHDC concept still has potential for further improvement. For instance, by lowering the distribution temperatures by including decentralized storage tanks for DHW combined with smart group charging [5] or by integrating decentralized booster heat pumps [6].

To fully exploit these advantages, proper design of the collective heating system is crucial where the first step is proper sizing of the system. Several studies [7], [8] show that sizing influences the performance of different heat production systems. In short, the main conclusion is that oversized systems often tend to decrease in energy efficiency due to poor part load behavior, while undersized systems result in a lack of comfort for the consumers. Moreover, sizing affects not only the production unit but also the distribution system, leading to higher heat losses and installation costs [9].

## 1.1 The design problem

In order to properly size the system, the heat demand at any point in the installation has to be determined. With respect to the design philosophy of the standard EN 12828 [10], the total required heat capacity for both SH and DHW-purposes of the system should be determined and calculated according to Equation 1.

$$\Phi_{SU} = f_{SH} \cdot \Phi_{SH} + f_{DHW} \cdot \Phi_{DHW} + f_{AS} + \Phi_{AS} \qquad (1)$$

Where, $\Phi_{SH}$ is the maximum heat demand for SH [kW], $\Phi_{DHW}$ the maximum heat demand for DHW production, and $\Phi_{AS}$ the maximum heat demand of any other attached systems, e.g. the heating coil of the centralized air handling unit. The factors $f_{SH}$, $f_{DHW,}$ and $f_{AS}$ take into account that on the one hand, $\Phi_{SH}$ and $\Phi_{DHW}$ are not the sum of the individual demands of the residential units for resp. SH and DHW, and on the other hand, the maximum heat demand of SH and DHW might not occur simultaneously.

In practice, these factors are often referred to as simultaneity or diversity factors. The existence and effect of the simultaneity phenomenon in collective heating systems were demonstrated in several studies. For example, Wang et al. [11] showed that due to simultaneity, the maximum total heat demand is reduced as opposed to the sum of the individual maximum demands. Furthermore, considering a good simultaneity factor in the calculation of the design heat demand, the risk of oversizing and the related disadvantages can be avoided [12].

However, within the Belgian context, currently, no standards or design rules exist for the sizing of collective two-pipe heating systems such as the CHDC and district heating. As a consequence, designers use a mix of foreign design guides and their own rules of thumb or manufacturers' specific design guides. In general, the following workflow is adopted by designers:

Firstly, the maximum collective heat demands for SH and DHW are calculated using the appropriate standards. Commonly, the standards for DHW already apply a simultaneity factor to account for the diversity in the DHW-heat demand. This simultaneity factor is generally determined based on either the number and type of tapping points or the number of dwellings connected to the heating network.

Secondly, the required total heat capacity is determined by combining the maximum heat demands determined in the first step through calculation rules. In practice, several approaches

exist: the summation approach, the maximum approach, and the weighted summation.

The summation approach, often used to avoid undersized systems, takes the sum of both heat demands for SH and DHW. While the summation approach is comprehensible when designing collective heating systems where both demands can occur simultaneously, this is not the case in collective heating systems such as the CHDC. In the CHDC and district heating systems, the end-users are usually connected to the primary network with a so-called flatstation or heat-interface unit (HIU). Generally, these HIUs cannot provide heat for SH and DHW-production simultaneously and thus work either in 'SH-mode' or 'DHW-mode', with a priority for DHW-demand. Consequently, the maximum heat demand for SH and DHW does not occur at the same time. As a result, applying the summation approach can lead to oversized systems.

Therefore, the maximum approach, which takes the maximum of both demands, is often used. The maximum approach is suitable for CHDC but depends on how the demands for SH and DHW are estimated. If the used standards overestimate these heat demand, then the maximum approach does not necessarily underestimate the heat demand. However, considering evolutions in the design standards for SH and DHW, the maximum approach can result in under-sizing problems. Especially in cases where the collective heat demand for SH does not differ much from the heat demand for DHW. To solve this issue, some engineering offices add 20% based on experience [13]. Nonetheless, this causes a lack of transparency.

The weighted average method calculates the total heat demand as the weighted sum of both heat demands (equation 2), where each heat demand is multiplied by a simultaneity factor. The factor $f_{DHW}$ is often the simultaneity factor according to the used standard to determine the DHW heat demand. The simultaneity factor for SH ($f_{SH}$) is calculated as ($1-f_{DHW}$) to cover worst-case situations. The physical explanation for this calculation is that the simultaneity factor for DHW estimates the maximum number of HIUs in 'DHW-mode', and thus in the worst case the other HIUs are in 'SH-mode'. This calculation rule is often used by German manufacturers of HIUs and is used in the German VDI 2072 standard [14].

$$\Phi_{SU} = (1 - f_{DHW}) \cdot \Phi_{SH} + f_{DHW} \cdot \Phi_{DHW} \qquad (2)$$

Although this calculation rule gives the most reasonable physical explanation, in practice the simultaneity factors as defined in the standards for DHW heat demand calculation are found to overestimate the heat demand. As a consequence, experimental simultaneity factors are mostly used, e.g. the simultaneity factor from TU Dresden [15], or simultaneity factors from other standards are combined. It is important to note that each simultaneity factor is defined based on different assumptions and constraints. As a consequence, improper mixed-use and comparison of standards and simultaneity factors cause a lack of transparency and reduce the general applicability of the sizing approach.

Furthermore, note that the mentioned calculation rules do not address the sizing of collective heating systems with central and decentral storage.

## 1.2 Method of maximum sum of parts

Based on the design discussion in the previous section, a new sizing method 'Method of the maximum sum of parts' was proposed [13]. The method aims to calculate the combined heat demand at any place in the collective heating system in a transparent way complementary to existing design standards for SH and DHW. This allows to easily integrate new insights in the determination of the SH and DHW demand.

### 1.2.1 Design Philosophy

The general philosophy of the method is to divide all residential units behind the investigated point of the system into two groups: 'space heating' or 'domestic hot water'. Thus, each dwelling is either divided into one of the two groups. Subsequently, the heat demand of each group is determined following the relevant standards for SH and DHW demand. Thereafter, the sum of parts is taken, i.e. the sum of the demand of both groups. As there are multiple ways to group the dwellings, the total heat demand is calculated for all possibilities, and the maximum of these calculations is retained as the required heat capacity to size the system.

As an illustrative example, the method is demonstrated for a simplified apartment building with 40 identical apartments. Each apartment has a SH heat demand of 3.5 kW, an average occupancy of 2.5 persons, and typical sanitary hot water equipment, comprising a bath or shower and three tapping points. According to the method, there are 41 possibilities to divide the apartments into the SH and DHW groups as they are all identical and not interfering. In Figure 1 the heat demand of each group is given as a function of the number of apartments in the group 'DHW'. The red curve presents the heat demand of the DHW-group, the blue curve of the SH-group, and the green curve presents the combined heat demand depending on the group distribution. According to the sizing method, the maximum of the green curve is retained as the required heat demand to which the installation must be sized. For the given example, the maximum heat demand for SH is 140 kW, the peak heat demand for instantaneous DHW production is 183 kW, and the maximum of 'the sum of parts' is 194.5 kW.

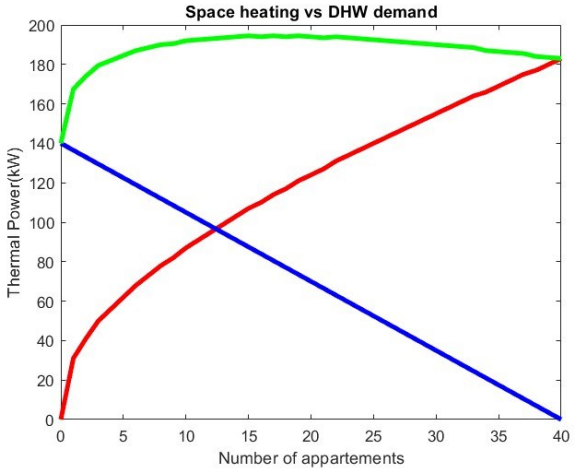


*Figure 1 Necessary heat demand for every group (blue for 'DHW' and red for 'SH') including their sum (green) as a function of the number of apartments dedicated to the group 'DHW'.*

### 1.2.2 Including the effects of thermal storage

In addition, the method is compatible with the power-storage method introduced by Verhaert et al. [16] making it possible to take the influence of the provision of thermal storage into account. Therefore, apart from variations in group division, also variations in thermal storage sizes are investigated. In this aspect, a third axis (Z-axis) is added to Figure 1 where the required power of the DHW group decreases with increasing

thermal storage capacity. A projection of the maxima of the Y-axis (Thermal Power) relative to this Z-axis yields a thermal power – thermal storage capacity characteristic, as presented in Figure 2. This characteristic represents the required central heat power as a function of the provided central heat storage capacity, is obtained.

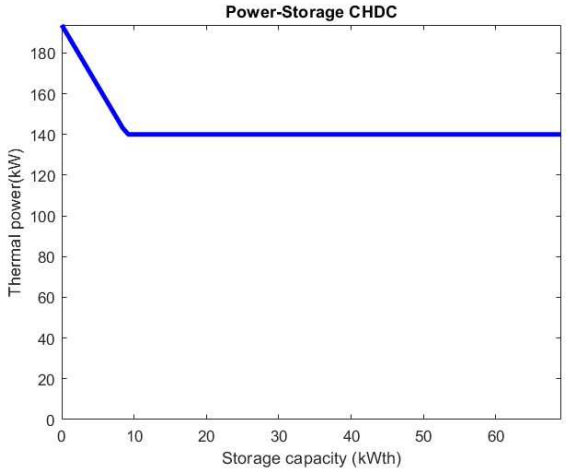


*Figure 2 'Thermal power - thermal storage characteristic' representing the possible combinations to cover the heat demand in a CHDC system.*

As can be noted, the required thermal power remains constant once a certain storage capacity is reached. By integrating the power-storage method of [16] into the method of maximum sum of parts, only the thermal storage's ability to lower the required thermal power for DHW is considered. This entails that from a certain thermal storage capacity the total required, i.e. the maximum of the green curve, will be defined by the maximum demand of the SH-group. Consequently, this allows the elimination of the gap between the maximum heat demand for SH and DHW production, preventing the system from being oversized most of the time with respect to the SH demand. Moreover, it is important to mention that the thermal storage should be regarded as 'active' thermal storage, which is the amount of heat (hot water) that is reserved as a backup when the thermal power of the heat production is temporarily too low to meet the current heat demand. Simplified, this is the water volume above the temperature sensor in the thermal storage tank that activates the heat production. Increasing the storage volume below the sensor does not reduce the required heating power but can help to reduce the cycling of the production unit or increase the share of renewable heat sources.

Furthermore, Verhaert [13] also proposed an approach to address the effect of decentralized thermal storage capacities in the design. In the case of collective heating systems such as the CHDC, the different dwellings can be connected with an HIU with a storage tank for DHW. Theoretically, these decentralized storage tanks also foresee some active thermal storage capacity which allows to lower the thermal power that is required centrally. To take the effect of the decentralized storage into account the following approach is suggested, i.e. to take the sum of all active decentralized storage into account as if the storage capacity is foreseen at the point in the installation where the heat demand needs to be determined. Once again, only active thermal storage is taken into account.

### 1.2.3 First assessment

Based on the first assessments in [13], [17] the approach of the maximum sum of parts shows potential. Compared to the simulations of case studies done in [17], the simulated heat demands align with the maximum approach and the maximum sum of parts. However, considering the previously mentioned findings of engineering offices, the maximum sum of parts approach offers more certainty and the required flexibility to evolve with new insights into SH and DHW design standards.

Furthermore, a comparison of the novel approach to the other methods was presented in [13]. Figure 3 presents an extension of this comparison to demonstrate how they relate to each other. The black line represents the maximum sum of part approach.

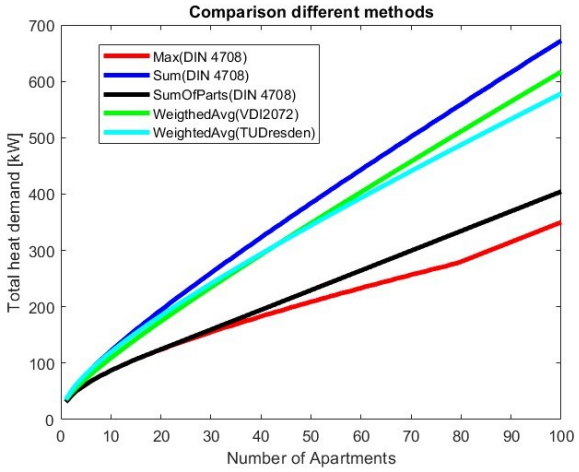


*Figure 3 Comparison of sizing methods, extending the findings of* [13]. *In parentheses the used standard to define the DHW demand and/or simultaneity factor.*

## 1.3 Scope of paper

The first assessments prove the potential of the sizing approach [13], [17]. However, it does not prove its validity. Therefore, this research aims to validate the approach by ascertaining its robustness and applicability. In this context, the utilization of authentic, real-world data becomes imperative. The use of real-world data rather than a simulation-based approach allows us to assess the design method for a diverse set of buildings with diverse types of occupants. This is at a relatively low cost compared to a simulation-based approach which can be information and time-intensive to obtain detailed physical models of the buildings and the occupant behavior. Therefore, the aim is to use heat consumption data obtained from residential (smart) heat meters to validate the new sizing method. The introduction of residential (smart) heat meters in collective heating systems, mainly used for billing purposes and monitoring, provides large datasets regarding heat consumption. However, some problems arise when using this type of data for the validation of sizing rules. More specifically, the poor data quality and the relatively large measurement interval pose some challenges. To reach the research objective, a validation methodology is presented to tackle these challenges, along with the results of the application of the procedure to six case studies.

# 2 The validation methodology

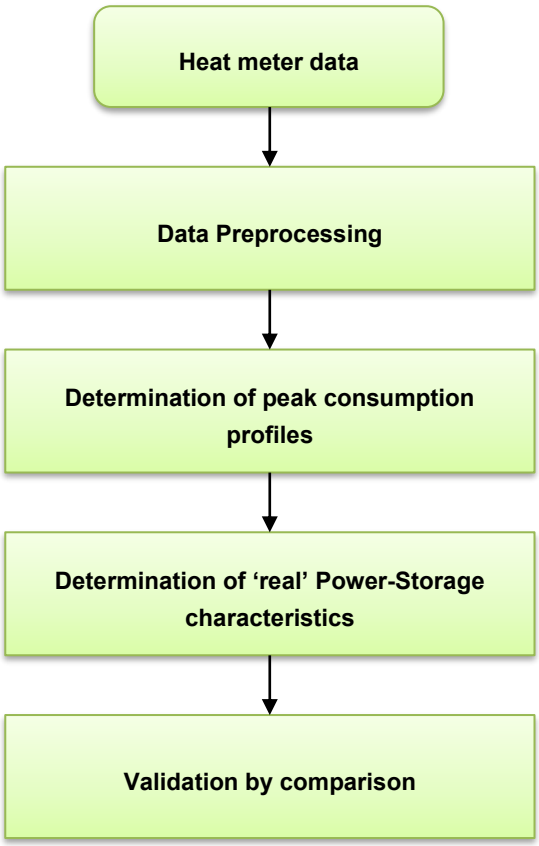


*Figure 4 General workflow of the validation methodology.*

## 2.1 Aim and Insights

The objective of the validation procedure is to compare the outcome of the 'method of maximum sum of parts' against the peak heat demand of the investigated case study. As previously mentioned, the outcome of the sizing method is a thermal power – thermal storage capacity characteristic (further called power-storage-characteristic) which presents all possible combinations of thermal power and storage capacity to satisfy the heat demand. To validate the sizing method, each combination needs to be able to cover the peak heat demand. Therefore, the validation methodology determines the 'real' power-storage characteristic needed to meet the peak heat demand using residential heat meter data.

The validation procedure is based on insights from the design methodology for DHW production systems of Verhaert et al. [16]. Based on tap patterns, they determined a worst-case consumption profile expressing the peak demand, i.e. volumes of hot water in liters, as a function of the duration of the measurement interval. Subsequently, by assessing the possible hot water production at a certain production capacity with respect to this profile, a production capacity – hot water storage characteristic is obtained.

However, there are challenges in using this method for the validation of the sizing rule. First, the data resolution and measurement frequency of residential heat meters, which often record cumulative heat consumption hourly in kilowatt-hours (kWh), must be considered. This can result in a lack of information on the peak heat consumption in smaller intervals and can significantly affect the determination of the 'real' power-storage characteristic. Second, the study examines the heat consumption of both DHW and SH, rather than DHW tap patterns. Because outdoor conditions influence SH consumption, they must be taken into account. Additionally, addressing the poor quality of residential heat meter data is crucial. To overcome these challenges, a validation methodology, presented in Figure 4, has been developed.

## 2.2 Resulted workflow

### 2.2.1 Data pre-processing

First of all, to cope with the poor data quality, the data is pre-processed. This step includes the standardization of the consumption according to fixed measurement times, the filling of missing values, and the removal of outliers. For the standardization and filling of missing data, linear interpolation is used. Other higher-order interpolation methods (e.g. cubic spline interpolation) were evaluated. However, these methods sometimes introduced oscillations and overshooting in the data, resulting in the introduction of significant erroneous values. Using linear interpolation may produce less accurate results, but may not affect the result of the validation. Whereas the use of higher-order methods does. Nevertheless, when data is missing for a long period (e.g. half a day), these periods are removed from the dataset. To simplify the identification and removal of outliers the variable 'the heat consumption per interval size' $\Delta Q(t)$ is determined. $\Delta Q(t)$, which is also used in further steps of the validation methodology, is derived from the cumulative heat consumption as follows:

$$\Delta Q(t) = Q(t) - Q(t-x) \tag{3}$$

Where Q(t) [kWh] is the registered cumulative heat consumption at time t and Q(t-x) [kWh] is the cumulative consumption at the previous measurement time point.

To remove outliers from the data different statistical methods were investigated: standard deviation around the (moving) mean and median, generalized extreme studentized deviation, and based on percentiles. The removal of outliers using an upper boundary defined by the 98-percentile of the daily maximum values of Q(t) has been found to give the most satisfying results. The large measurement interval, being fifteen minutes up to one hour, caused the removal of too much valuable data when using the other mentioned methods.

Furthermore, for validation purposes, only data from representative residential units must be included. It is often possible that some apartments are vacant or become vacant, or faults may be present. This can affect the result of the validation in favor of the design method. In this aspect, the data from each heat meter was analyzed, and general characteristics such as the average and maximum daily peak heat load, the number of days with consumption above a certain threshold, and the total heat consumption over the measurement period. Based on the manual inspection of these characteristics threshold criteria are defined to determine which heat meters can be included in the analysis.

### 2.2.2 Determination of the Peak Consumption Profile

As mentioned before, similar to the approach of Verhaert et al. [16] to obtain power-storage characteristics from DHW-tap profiles, a worst-case or peak consumption profile is determined from the heat consumption data. This profile represents the maximum cumulative heat demand that can occur during a specific time or measurement interval x and is defined using Equation 4:

$$C(x) = \max(\Delta Q(t), \forall t) \quad (4)$$

However, the measurement interval size of the heat meters prevents the determination of the complete profile as the data for small intervals are lacking. To deal with this problem, at first, the average heat capacity or power Φ(x) required to cover the maximum heat consumption that can occur within a specific time or measurement interval size x is determined. This average power Φ(x) is determined as follows:

$$\Phi(x) = \max\left(\frac{\Delta Q(t)}{x}, \forall t\right) \quad (5)$$

This graph allows to identify a so-called 'critical interval'. During this critical interval, as the measurement interval size increases, the average power remains more or less constant. Also, the largest interval size for which this average power is barely affected can be an indication of the duration of the peak heat demand. Since the demand is collective, the peak heat demand may occur for a longer time. The existence of such an interval for DHW consumption was addressed by Verhaert et al. [16]. Also, the study of Wang et al. [11] showed that when examining collective heat consumption data from a district heating network, data with a half-hourly to hourly measurement frequency is sufficient enough to identify the peak heat demand. This indicates that it may be possible to identify a critical measurement interval for collective heating systems that provide both heat for SH and DHW purposes.

If such a 'critical interval' can be observed, it can be concluded that the maximum average power Φ(x) of the smallest measurable interval size is representative for interval sizes below the actual measurement interval size. Consequently, this solves the problem of the relatively large measurement interval size. Nevertheless, the critical interval might be shorter than the measurement interval of the heat meters. When this is the case, the peak consumption profile is filled using an approximation equation. Given that the peak consumption profile is an ever-increasing curve, and taking into account the observations of Verhaert et al. [16], a second-order degree polynomial equation is assumed to be a proper approximation.

$$A(x) = a \cdot x^2 + b \cdot x + c \quad (6)$$

The coefficients can be determined based on the following: As no consumption exists during a time interval of zero, c is zero. Furthermore, coefficients a and b can be determined given that, on one hand, the value of C(x) and A(x) should be the same for the smallest known value of x, and on the other hand, the slope of the tangents at this point must also be equal.

Using this approximation the problem of the measurement frequency is solved. Nonetheless, another challenge to account for is the fact that systems for space heating are sized based on certain outdoor design conditions. According to the standard EN 12831-1 [18], the design heat load is calculated at a location-specific external design temperature. Since the outcome of the design tool depends on this calculated design heat load, the peak consumption profile has to be determined at design outdoor conditions for proper validation. However, it is possible that these design conditions may not occur during the measurement period. Therefore, a method is defined to estimate the peak load profile at design outdoor conditions.

Various methods exist to estimate the heat consumption, with linear regression models being common. In the simplest form, this involves energy signature models, using outdoor temperature as the sole independent variable and daily or monthly heat consumption as the dependent variable [19]. More complex multivariate regression models incorporate additional independent variables, including building parameters [20], other outdoor climate factors [21], time-related variables, and historical data from previous time steps [22]–[25]. More recent approaches include autoregressive models [26], support vector machines (SVM), and artificial neural networks (ANN) [24], [25], mainly for predicting near-future heat loads, often for the next 24 to 42 hours. These models use predicted climate variables, time-related factors, and historical climate and heat load data over various time horizons, typically ranging from 24 hours to one week. Based on the results of [24] and [25], ANN-models gave the most accurate predictions in the case of building heat load estimation.

Given the research objective of estimating the peak consumption profile at design conditions, using the aforementioned methods presents challenges. Often the standards to calculate the design heat load for SH only provide a certain design outdoor temperature. Thus, climate conditions of the preceding time horizon, which are used as inputs in the models, are undefined. Defining these inputs is complex and will require additional research, which is out of the scope of this research. Nonetheless, it is possible to investigate the application of ANNs, SVMs, and other machine-learning models without historical inputs. However, the limited availability of heat consumption data and expertise in this study constrains the development and comprehensive evaluation of such models. Therefore, the use of a multivariate linear regression model was opted. The linear regression model is derived from the energy balance equation. This approach provides transparency in analyzing the models output against the actual data, allowing to incorporate a conservative safety margin to account for the inaccuracies in the determination of the peak consumption profile due to the model under-specification.

The energy balance of the heat demand in a CHDC system is the result of two sub-demands, i.e. the heat demand for SH and the heat demand for DHW preparation. The heat demand for SH during a certain time interval can be defined using Equation 7. The parameter L is a linear loss factor including factors such as the thermal insulation rate, building materials, ventilation losses (depending on the used ventilation system), and air leakage. Parameter C is a lumped capacitance taking into account the thermal inertia of the building and heated space. The term S·I represents the solar heat gains with S the solar heat gains coefficient, which can be perceived as the solar aperture, and I the solar radiation in Wh/m².

$$Q_{SH} = \int L \cdot (T_i - T_o)\, dt + \int C \cdot \frac{dT_i}{dt}\, dt - S \cdot I - Q_{int,gain} \quad (7)$$

In this way, the balance of the total heat demand is given as follows:

$$Q_{tot} = \int L \cdot (T_i - T_o)\, dt + \int C \cdot \frac{dT_i}{dt}\, dt - S \cdot I - Q_{int,gain} + Q_{DHW} \quad (8)$$

While incorporating windspeed effects may enhance the fit, it is not considered in this research, as it focuses exclusively on recently constructed buildings compliant with Belgian building regulations. If older buildings were included, we could introduce a windspeed factor into Equation 8.

Due to the lack of information on the buildings, data regarding the occupant behavior and the actual indoor air temperature, parameter C, the internal heat gains, and the domestic hot water demand cannot be derived or estimated from the consumption data. Therefore, Equation 8 is compared with

the general equation of a linear regression model with the outdoor temperature and the solar radiation as independent variables, which is given as:

$$Q = \beta_0 + \beta_1 \cdot T_o + \beta_2 \cdot I + \varepsilon \quad (9)$$

Based on this comparison, it is possible to relate the coefficients of Equation 9 to the parameters of Equation 8. This, in turn, allows to infer that the intercept and the deviations between the regression model and the real consumption data can be related to the dynamic effects arising from the thermal inertia, variations in the indoor air temperature, the internal heat gains, and the DHW demand.

$$\int \mathrm{L} \cdot T_i \, dt + \int \mathrm{C} \cdot \frac{dT_i}{dt} \, \mathrm{dt} - Q_{int,gains} + Q_{DHW} = \beta_0 + \varepsilon \quad (10)$$

The intercept $\beta_0$ will represent the mean value of the sum of these terms, and the error term $\varepsilon$ the deviations from this mean. Given that these terms are dependent on the occupant behavior and have a high stochastic nature, especially the internal heat gains and the DHW demand, the model is not able to accurately predict the peak consumption profile and is likely to underestimate the profile. To cope with this, the maximum positive error between the model prediction and the actual measured heat consumption is calculated and added to the model predictions at worst case or design outdoor conditions. Furthermore, based on previous analysis of heat consumption data, the maximum positive error will not be determined over the entire temperature range but only for a specific range (i.e. for outdoor temperatures lower than four degrees Celsius) since it is assumed that the terms related to the error will have some seasonal dependence.

Nonetheless, as mentioned by Hammarsten S. [21] and Himpe E. et al. [26], the use of data with a measurement frequency lower than 24 hours for the fitting of the regression model is not recommended as it may lead to inaccurate models. The main reason is the fact that the data is autocorrelated due to intra-daily effects in both the outdoor climate, the physics of the building and the installation, and the user behavior. For example, if the heating system follows a time-based control and the users behavior follows a certain pattern, the heat demand can differ from hour to hour and affect the heat demand of consecutive hours. This is often seen in the analysis of heat load patterns of buildings [19], [27]. Therefore, the time of the day (ToD) is included in the regression model to take these effects into account. As a result, the coefficients and the intercept of the regression model are dependent on the time of the day.

$$Q = \beta_0(ToD) + \beta_1(ToD) \cdot T_o + \beta_2(ToD) \cdot I + \varepsilon \quad (11)$$

Furthermore, based on the results of Himpe E. et al. [26] replacing the average outdoor temperature with the daily heating degrees days (HDD) provides a better fit since it helps to account for the effect of heat gains and the thermal inertia of the building [28]. Therefore, an alternative regression model including the daily heating degree days is foreseen, where the daily number of degree days is determined in accordance with the method according to the Belgian Gas Federation [29].

$$Q = \beta_0(ToD) + \beta_1(ToD) \cdot HDD + \beta_2(ToD) \cdot I + \varepsilon \quad (12)$$

Depending on the outcome of the fitting analysis, either the model based on the outdoor temperature or the daily number of degree days will be used to determine the peak load profile at design conditions. In the event that the model based on the outdoor temperature yields the best results, the peak load profile is estimated at the design outdoor temperature, defined following the EN 12831-1 standard [18]. Conversely, in the other scenario, the problem that there is no such concept as "design number of heating degree days" arises. Consequently, a pragmatic approach is adopted, where the maximum daily heating degree days of the last 10 years is used to define the worst-case conditions.

To conclude, the peak load profile is determined in two ways: once based on the effectively measured heat consumption, and once at design or worst-case conditions using the aforementioned method based on linear regression models.

### 2.2.3 Determination of the 'real' power-storage characteristic

Once the peak consumption profile is determined, both based on the measured heat consumption data and estimated at design conditions, the 'real' power-storage characteristics can be determined. By comparing the possible heat production P(x) that a certain production capacity can provide within a certain time interval with respect to every point on the peak consumption profile, the required thermal storage $Q_{stor}$ can be derived as follows:

$$Q_{stor} = max\big(C(x) - P(x)\big) \quad (13)$$

The process is graphically shown in Figure 5. As long as the possible heat production is greater than the peak demand C(x), no thermal storage is required to cover the peak heat demand.

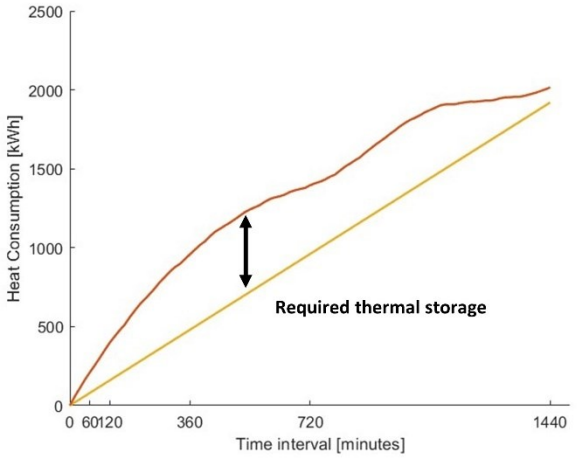


*Figure 5 Evaluation of the possible heat production of a certain thermal capacity P(x) (yellow line) against the peak consumption profile C(x) (orange line). The maximum positive difference between C(x) and P(x) gives the required thermal storage.*

By evaluating a range of production capacities, the required thermal storage can be plotted as a function of the foreseen production capacity. As a result, this graph represents the 'real' power-storage characteristic which shows the possible combinations of production capacity and thermal storage required to meet the peak heat demand. The 'real' power-storage characteristic is determined based on the peak consumption profile measured as well as the one estimated at design or worst-case outdoor conditions.

### 2.2.4 Comparison of characteristics

As presented in Figure 6, in the final step of the validation methodology, the resulting power-storage characteristics are compared with the outcome of the sizing method. The characteristics derived from the measurement data show the minimum required combinations to meet the peak heat demand within the time interval ranging from 0 to 1440 minutes. All possible combinations above these characteristics will provide comfort. Conversely, combinations below these characteristics result in discomfort. Thus, to prove the validity of the sizing approach, the resulting characteristic should deliver higher or equal combinations to the characteristics derived from the measurement data.

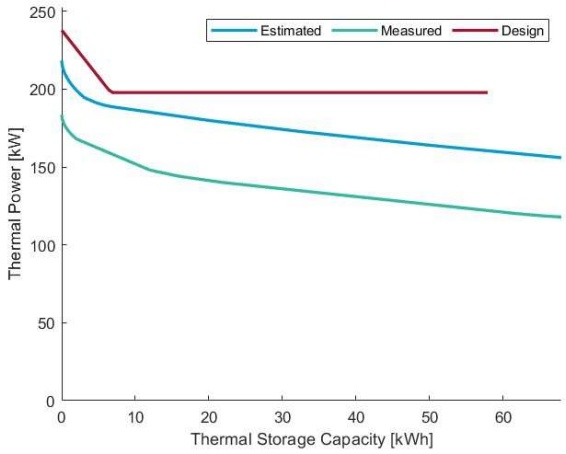


*Figure 6 Comparison of power-storage characteristics, red the output of the sizing method, blue the estimated characteristic, and green the actual measured characteristics.*

## 2.3 Case studies

The validation methodology is applied to six case studies. All of the buildings are located in Antwerp, Belgium. Four of the buildings (buildings B to E) are part of a new city district in the city of Antwerp and are connected to a district heating network. The two other buildings, A and F, are located in rural areas to the north and the west of the city of Antwerp respectively, and have their own centralized heat production. The general characteristics of the buildings are presented in Table 1. The insulation rate of the buildings is presented through the 'K-peil', which is an indication of the overall thermal insulation of the building as defined by the Flemish energy performance regulations for buildings (EPB) [30]. All of the case studies are equipped with a CHDC system for the distribution of heat to each apartment unit. In buildings A to E, the apartments are equipped with an HIU with a plate heat exchanger for the instantaneous production of DWH. In building F the apartments are equipped with an HIU with a decentral storage tank of 60 liters with an internal heating coil. Buildings C to F use radiators as their heat-emitting system, whereas buildings A and B are equipped with floor heating.

Furthermore, all of the apartments are equipped with a smart heat meter which records the cumulative heat consumption. Normally, the heat consumption is registered on an hourly or daily basis. However, for this research, the registration frequency was adjusted to a quarterly basis, except for building B where the frequency was kept on hourly basis by the building operator. Due to the adjustment of the registration interval, and agreements with the building owners, data is only available from November 2020 to May 2021, except for Building F where data is available for the period from November 2020 to November 2021. Since the outdoor conditions are not measured at each building, climate data is used from the weather station of the Royal Meteorological Institute of Belgium located in the city of Antwerp [31] or data from a weather station located in the north of the province of Antwerp [32]. Depending on the location of the case, data from the nearest weather station is used.

As mentioned in the introduction of the sizing method, the first step in sizing is to determine the separate heat demand for SH and DHW. Table 2 shows the inputs for the sizing method, along with the registration interval of the heat consumption data for each case study. Preliminary results showed the best results when combining the sizing approach with the German DIN 4708 standard [17].

# 3 Results and Discussion

## 3.1 Results of the data pre-processing

As mentioned in Section 2.2.1, we initially assess the eligibility of individual apartment units for inclusion in the validation study. This evaluation is primarily based on a visual inspection of their total and average daily heat consumption and the number of days with heat consumption. For building A, 33 out of 59 apartments were deemed eligible. Building B had 33 eligible apartments, while building C had 14, Building D and E had 19 and 7, respectively.

## 3.2 Identification of the critical interval

Figure 7 shows the average power needed to meet peak heat demand based on measurement interval size for the analyzed case studies. The average power remains fairly constant from 720 to 1440 minutes but rises sharply for intervals less than 120 minutes. However, the absence of a flattening trend suggests that the critical interval is below fifteen minutes. Consequently, following the validation methodology, an approximation equation was applied to fill the peak consumption profiles.

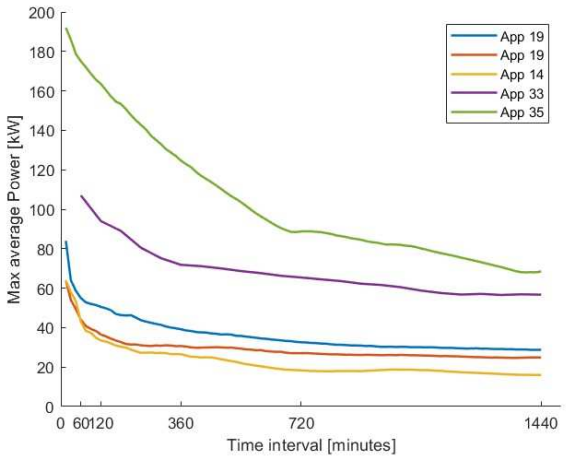


*Figure 7 Average power required to cover the peak consumption with respect to the measurement interval size x.*

*Table 1 Building characteristics of the case studies.*

| Building | # apartments | Type | Insulation rate (K-peil) | Floor area | Space Heating and sanitary equipment |
|---|---|---|---|---|---|
| **A** | 59 | Normal service flats | 31 – 33 | 56 – 119 m² | Floor heating<br>Bad or shower, 1-3 taps |
| **B** | 47 | Normal<br>4 maisonettes | 40 | 49 – 140 m² | Floor heating<br>Bad and/or shower, 1-3 taps |
| **C** | 16 | Normal | 40 | ± 60 m² | Radiators<br>Bad or shower, 1-3 taps |
| **D** | 25 | Social housing | 40 | 60 – 120 m² | Radiators<br>Bad or shower, 1-3 taps |
| **E** | 30 | Social housing | 40 | 60 – 120 m² | Radiators<br>Bad or shower, 1-3 taps |
| **F** | 8 | Social housing | 30 | 75 – 90 m² | Radiators<br>Shower, 1-3 taps |

*Table 2 Building and occupant characteristics used as input for the sizing approach along with the available measurement interval.*

| Building | Occupancy (DIN 4708) [persons] | DHW-demand (DIN 4708) [Wh] | SH-demand [kW] | Measurement interval [minutes] |
|---|---|---|---|---|
| **A** | 2 – 3.5 | 5820 | 4.5 – 9.6 | 15 |
| **B** | 2 – 3.5 | 5820 – 7450 | 2.5 – 7.0 | 60 |
| **C** | 2 – 2.7 | 5820 | 2.5 | 15 |
| **D** | 2 – 4.3 | 5820 | 2.9 – 4.3 | 15 |
| **E** | 2 – 4.3 | 5820 | 2 – 3.5 | 15 |
| **F** | 2 – 2.7 | 5820 | 3.1 – 3.5 | 10 |

## 3.3 Linear regression model fitting results

The fitting results of the linear regression model are presented in Figure 8. The graphs show for each case study the $R^2$-values (adjusted) of the model fit for each measurement interval size. First of all, it can be noted that for all of the cases, the models based on HDD provide the best fit, as they have higher $R^2$-values. This is in accordance with [27] due to the better identification of the effect of heat gains, thermal inertia, and seasonality.

Besides, it can be observed that the regression model exhibits the weakest performance for the smallest interval sizes. The $R^2$-values for the shortest measurement intervals between 15 and 60 minutes range between 0.27 and 0.44. Except for Case A, where the $R^2$-value for the smallest interval size is 0.88. The low accuracy of the regression model for small interval sizes is due to two effects. First, the heat demand of DHW influences the accuracy at low intervals, as this heat demand is of relatively short duration and a stochastic nature. Second, the accuracy is influenced by the control and the type of space heating system, given that all the HIUs are controlled by an ON/OFF signal from the thermostat. This control lacks modulation based on the outdoor temperature, and combined with the prolonged time constants of the space heating system, causes the space heating system to operate at maximum load, regardless of the outdoor temperature. Both effects affect the heat consumption during small interval sizes which results in a nonlinear correlation between the heat consumption and outdoor temperature or HDD.

This phenomenon is also visible in the graphs showing the maximum average peak power as a function of the measurement interval size and the outdoor temperature. Examples are given in Figure 9 for Cases C and E. As can be seen, the average power to meet the peak heat demand at low intervals increases when the outdoor temperature decreases. However, the increase in average power is not linear with the outdoor temperature, and the maximum average power is not requested at the lowest outside temperature.

Nonetheless, case A seems to be the exception. A possible explanation is the presence of a central night setback, as the central heat production system is switched off from 00:00 to 04:00. This night setback creates a very pronounced and long morning peak where the effect is intensified by the use of floor heating as SH system. In combination with a low relative share of DHW in the total heat consumption, this makes the heat consumption strongly correlated with the outdoor temperature, thus providing better fit results. In addition, it is worth mentioning that this type of control is not advisable in CHDC systems, as the temperature reduction inhibits the decentralized production of DHW at the individual HIUs and results in prolonged periods of discomfort owing to the extensive waiting times for the reheating of the spaces when floor heating is used.

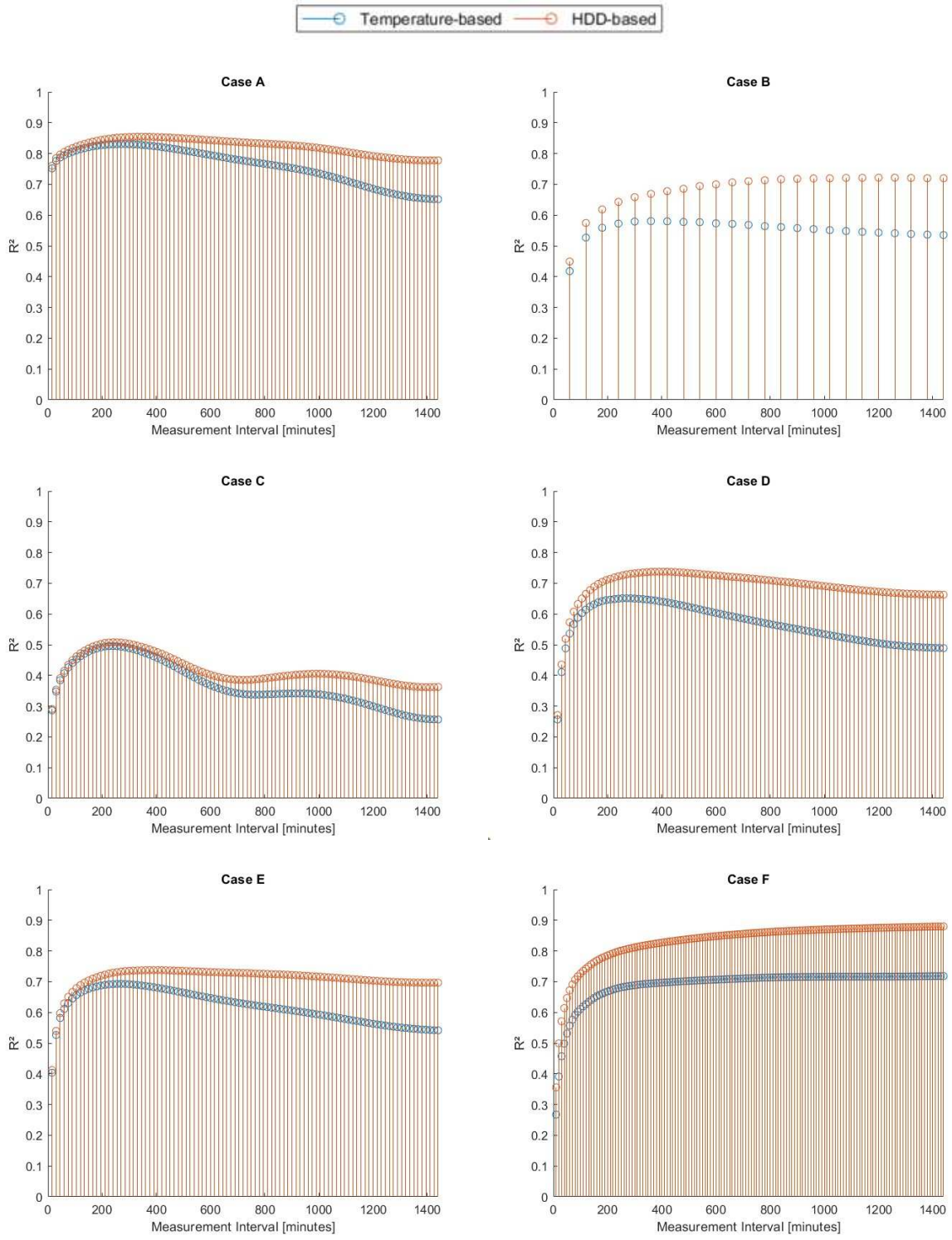


*Figure 8 Fitting results of the linear regression models for each measurement interval size, indicated by R² (adjusted) values. Orange: the results of the models based on HDD. Blue: the results of models based on the daily average outdoor temperature.*

Furthermore, starting from the smallest time interval, it is notable that, as the measurement interval increases, the R²-values improve until a point where they start to decrease. This contrasts with the expectation that the fit improves and stabilizes as the measurement interval size increases. Especially when looking at Cases A, C, D, and E, it can be observed that the R² values improve up to a measurement interval size of 245 to 390 minutes and then decrease again until the values finally more or less stabilize towards the larger measurement interval sizes (>800 minutes). The variability in the fit results is thought to be attributed to a combination of factors related to the occupant behavior and the space heating system operations. This is mainly derived from the findings of Case C, where this pattern is most pronounced. In the instance of Case C, there is a significant share of DHW in the total heat demand. The occupants are comprised of working families which most likely follow a conventional daily routine consistent with that of working individuals. Consequently, the space heating system is

often controlled through a time-based control, i.e. a reduction in the room temperature during periods of absence and throughout the night. As a result, a typical daily heat load pattern emerges with morning and evening peaks attributed to the start-up of the space heating system and the more grouped DHW demand following the daily usage patterns typical of a working individual.

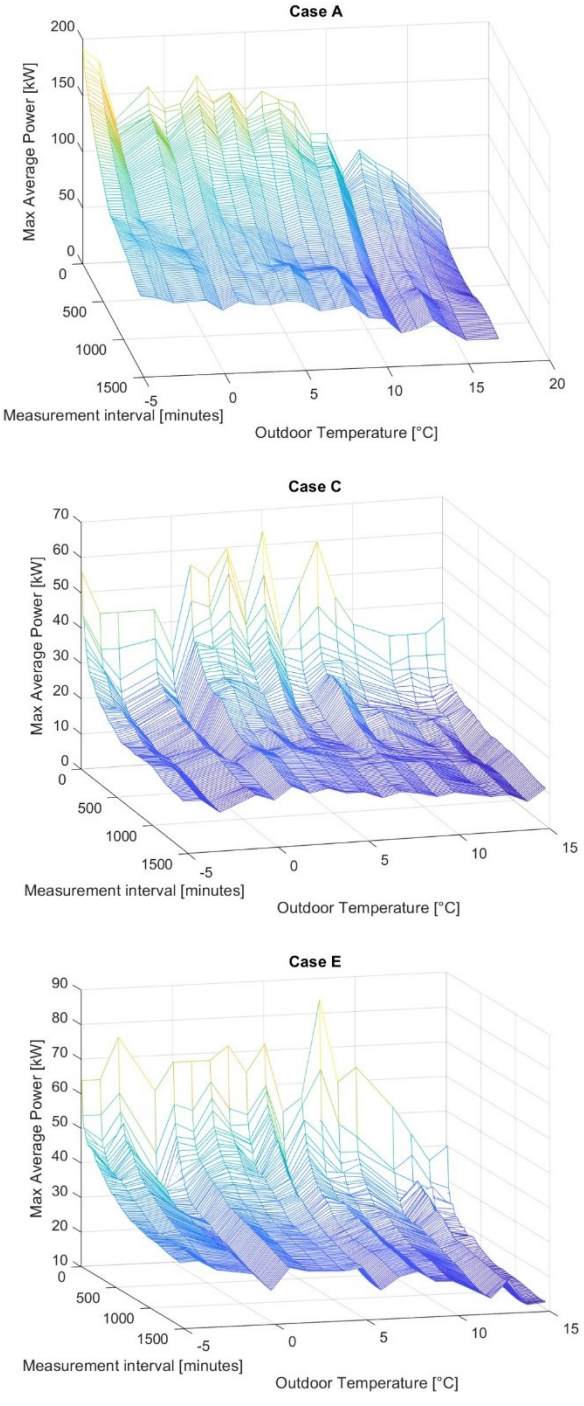


*Figure 9 Average peak power as a function of the measurement interval size with respect to the outdoor temperature.*

It is hypothesized that, on one hand, this contributed to the lower fit results for smaller interval sizes as discussed earlier. On the other hand, the time-based control of the SH system leads to high startup peaks and further categorizes the heat consumption into periods of increased demand when the SH system is active, and periods of reduced demand when the system is in setback mode. Typically, these periods when the system is active span around 3 to 5 hours. As a result, the heat consumption over these periods becomes more strongly correlated with the outdoor temperature or the number of degree days, resulting in a better fit. As the measurement interval increases, the 'active and setback' periods start to overlap, and the heat consumption is more averaged out. Additionally, the proportion of DHW in heat consumption increases over the measurement period due to diversity in the demand. These combined factors lead to a decrease in $R^2$-values as the measurement interval increases and gradually appears to stabilize.

For Cases A, D, and E, the previously discussed pattern in the $R^2$-values is also visible but less pronounced. In these cases the share of DHW in the total heat demand is relatively lower, partly owing to the nature of the buildings, which falls under the category of social housing. Furthermore, the occupants of these cases predominantly consist of elderly and persons whose daily routines diverge from the daily routines of the typical working individuals. Consequently, this leads to a heat load pattern corresponding to their habits. These factors likely contributed to milder fluctuations in the observed $R^2$-values compared to Case C.

Nevertheless, it is important to note that these findings are only based on a limited number of case studies. To draw definitive conclusions, further research including more case studies, is necessary.

## 3.4 Results of the validation methodology: comparing characteristics

Following the validation procedure, once the peak consumption profile is determined both based on the actual measured heat consumption and estimated using the extrapolation methodology based on a multivariate linear regression, the 'real' power-storage characteristics are derived. Since the evaluation of the regression models showed that the ones based on HDD performed better than the ones based on the daily average temperature, HDD-based models were used to determine the peak consumption profile. For the analyzed case studies the worst-case scenario corresponds with 25 degree days [29].

The results of the application of the validation methodology to six case studies are presented in Figure 10. In the figure, the green curves represent the power-storage characteristics based purely on the measured heat consumption, and the blue curves represent the ones based on the estimated heat consumption at worst-case conditions. The dark red and orange curves represent the output from the sizing method. Due to privacy reasons, it was not possible to find out which apartments were excluded from the validation study. Therefore, two different outputs were calculated according to the sizing method. Once for the 'n' number of apartments with the highest design heat demand for SH and DHW, presented by the dark red curve, and once for the 'n' apartments with the lowest heat demand, presented by the orange curve. Where 'n' equals the number of apartments included in the validation study.

Looking at the results of cases A to E, it can be observed that the output of the sizing method lies above the power-storage characteristics based on the heat consumption data. Subsequently, this shows that the output of the sizing method is capable of covering the peak heat demand. Furthermore, as can be seen, an uncertainty boundary is included, presented by the grey line. This uncertainty boundary is the result of using the

approximation equation to fill the peak consumption profile for intervals below the minimum measurement interval available in the data. All points of the real power-storage characteristics at the left of this uncertainty boundary result from this approximation, and therefore, cannot be fully validated to cover the peak heat demand. Nonetheless, these points of the characteristics are mainly defined by instantaneous peak heat demands which are strongly influenced by DHW heat demand with a base heat demand for SH. However, as seen in the heat consumption data, the peaks resulting from the DHW demand are highly dependent on the chance of the simultaneous demand for DHW by all of the apartments, and the occurrence of these peaks is limited. As a result, from an economic perspective, it is more interesting to size the central heat production system based on the point where the design power-storage characteristic 'flattens'. As can be seen in the results, for the case studies with data measured at intervals of 15 minutes or less, this point lies to the right of the uncertainty boundary, thereby confirming its validity. For cases A, B, D, and E, the point where the design characteristic flattens lies above the real power-storage characteristics. However, case C reveals a minor discrepancy of 0.4 kW between the sizing method's output and the measured power-storage characteristic. In reality, however, this small discrepancy is likely to be compensated for by the effective selection of the heat production and storage equipment, along with any supplementary power allocated to cover distribution losses.

As shown in Figure 10, the graph of case F shows some differences from the graphs of the other cases. More specifically, the real power-storage characteristics have undergone a rightward shift. This owes to the fact that in the instance of Case F HIU's with decentralized storage tanks are used. As mentioned in the explanation of the sizing method in the Introduction, due to the presence of the decentralized storage tanks, there is already some active thermal storage. This decentral storage reduces the peak power required from the central heat production and thus needs to be taken into account. Therefore, the total decentralized active storage capacity is calculated and added to the real power-storage characteristics. As a result, these characteristics shift rightward, and subsequently, allow to compare the characteristics to the design characteristic.

As can be noticed, in the instance of case F, the design output falls under the real power-storage characteristics, indicating that the design according to the sizing method will not be able to cover the peak heat demand. An explanation was found in the use of the DIN 4708 standard for the calculation of the heat demand for DHW. To determine the heat demand for DHW that occurs within a specific period, the German standard derives a Gaussian normal distribution of the heat demand based on the number of dwellings and the sanitary equipment. However, the parameters used to establish this normal distribution assume an instantaneous consumption of DHW. The presence of the decentralized storage affects the shape of this normal distribution, due to inter alia the accumulation of the domestic hot water demand. Moreover, the charging flow rates set to charge the decentral storage tanks influence the peak heat demand, as has been demonstrated by Jacobs et al. [5]. As these influences are not accounted for by the DIN 4708 standard, the intended physical significance is lost, and subsequently, the output of the sizing method may result in inaccurate sizing.

Finally, the accuracy of the approaches used to deal with the limited accuracy and resolution inherent in the data from residential heat meters was also investigated. On the one hand, the accuracy of the most recent heat meters is acceptable for the objective of this study. On the other hand, the resolution at which the heat consumption is calculated and recorded by the heat meters can cause concern. In most cases, the heat consumption is recorded on a kWh basis. This rather low resolution can lead to an underestimation, especially when the data from multiple heat meters are accumulated. On the contrary, also an overestimation is possible. To verify whether the peak thermal power determined by the approximation equation specified in Section 2.2.2, differs significantly from the real measured peaks, the instant power was determined from the heat meter data. The instantaneous power was calculated from the heat meter data by using the temperature and flow measurement data, according to the calculation methods specified by the NBN EN 1434-1:2015 [33], concerning the general requirements of thermal energy meters. Subsequently, the calculated thermal powers of all heat meters are summed and the maximum is calculated. The total thermal power is then compared with the results of the approximation method.

Table 3 presents the actual measured and approximated instantaneous thermal power for all the cases. Apart from case E, there is generally no significant over or underestimation. However, since the actual measured instantaneous thermal power is calculated from measurements with quarter-hourly to hourly measurement frequency, the possibility exists that the actual peak power is not captured. Nevertheless, the comparison offers insights into the alignment and relative magnitudes of the measured and approximated peak power values.

*Table 3 Comparison between the measured instantaneous peak power and instantaneous peak power according to the peak consumption profile.*

| | **Peak Power – instant measured [kW]** | **Peak Power – approximation [kW]** |
|---|---|---|
| **Case A** | 194.2 | 203.2 |
| **Case B** | 125.7 | 132.6 |
| **Case C** | 75.6 | 75.2 |
| **Case D** | 73.0 | 82.7 |
| **Case E** | 89.0 | 121.3 |
| **Case F** | 56.1 | 52.8 |

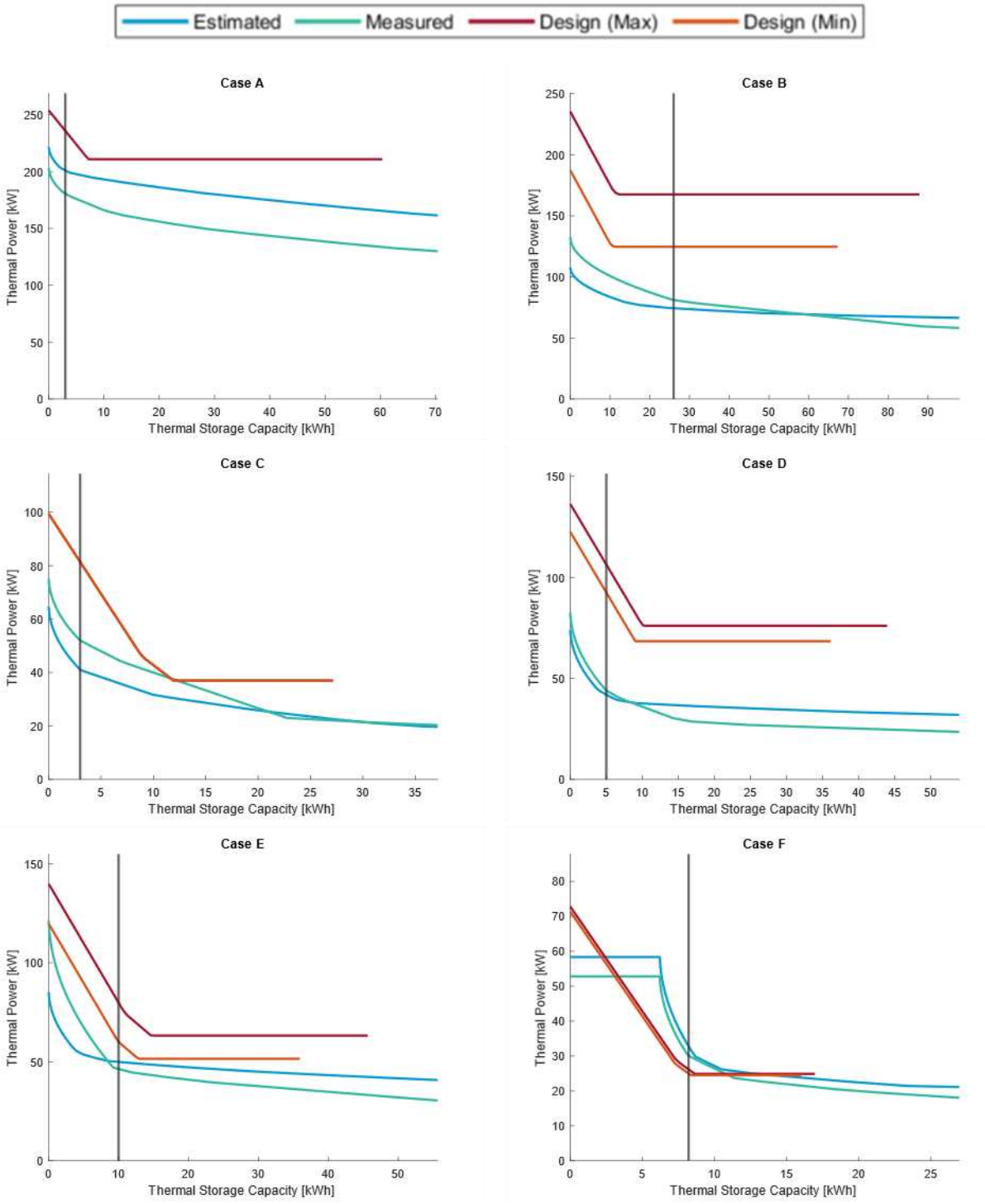


*Figure 10 Comparison of power-storage characteristics. Red and orange: the characteristics according to the maximum sum of parts. Blue: the characteristic estimated at worst-case outdoor conditions. Green: the characteristic based on the actual measured heat consumption*

# 4 Conclusion

In this paper, a validation methodology is presented to validate a novel sizing approach for collective systems that produce and/or distribute heat for space heating and domestic hot water. The validation methodology was developed to overcome the limitations associated with residential heat meter data, such as the limited measurement frequency and resolution. It involved the derivation of a peak consumption profile from heat consumption data and an estimation of this profile under worst-case outdoor conditions, which might not be present in the data. A multivariate regression model, coupled with an analysis of the maximum deviations, was employed to determine the peak consumption profile under worst-case outdoor conditions. Subsequently, the peak consumption profile enables the determination of the power-storage characteristics, which represents all possible combinations of thermal power and storage capacity required to meet the measured or estimated peak heat demand. In turn, this power-storage characteristic is compared to the output of the sizing approach.

Analysis of the peak consumption profile and evaluation of the fitting results demonstrated that the peak consumption over shorter intervals (15 to 60 minutes) is predominantly influenced by the DHW consumption and whether the SH system is active or not. The actual outdoor temperature plays a lesser role, although this depends on factors such as location, occupant type, and control strategy. The peak consumption over longer intervals showed an increasing correlation with decreasing outdoor temperatures.

The validation methodology was applied to six case studies, focusing on apartment buildings with a collective heating system of the CHDC type. The results demonstrated that for apartment buildings equipped with HIUs for instantaneous DHW production, the sizing approach is capable of covering the peak heat demand both measured as predicted at worst-case outdoor conditions. Nevertheless, the results show that in the case where decentralized DHW storage tanks are present, the sizing approach may result in under-sizing. This discrepancy primarily arises from the incompatibility of the prescribed approach for including decentralized storage into account in the sizing and the German DIN 4708 standard, which is used to determine the DHW demand. Consequently, further research is necessary to adapt the sizing approach to ensure its applicability and accuracy for the sizing of collective heating systems with decentralized DHW storage


## Acknowledgments

The authors gratefully acknowledge the funding provided by Flanders Innovation and Entrepreneurship, the city of Antwerp and Fluvius. as well as the feedback of the consortium of Flemish companies supporting the project.


## Disclosure statement

The authors report there are no competing interests to declare.


## Funding

This research was funded by Flanders Innovation and Entrepreneurship (VLAIO) [HBC.2019.2020], and the Heat Networks chair funded by the City of Antwerp and Fluvius.


## Data availability statement

The data used in this study are available from the corresponding author upon reasonable request.


## ORCID

Senne Van Minnebruggen https://orcid.org/0000-0002-8215-733X
Houssam Matbouli https://orcid.org/0000-0002-9402-3945
Stef Jacobs https://orcid.org/0000-0001-8179-3468
Ivan Verhaert https://orcid.org/0000-0002-5238-6123


## References


[1] H. Lund *et al.*, "4th Generation District Heating (4GDH): Integrating smart thermal grids into future sustainable energy systems," *Energy*, vol. 68, pp. 1–11, Apr. 2014, doi: 10.1016/J.ENERGY.2014.02.089.

[2] D. Connolly *et al.*, "Heat Roadmap Europe: Combining district heating with heat savings to decarbonise the EU energy system," *Energy Policy*, vol. 65, pp. 475–489, Feb. 2014, doi: 10.1016/J.ENPOL.2013.10.035.

[3] X. Yang, H. Li, and S. Svendsen, "Decentralized substations for low-temperature district heating with no Legionella risk, and low return temperatures," *Energy*, vol. 110, pp. 65–74, Sep. 2016, doi: 10.1016/J.ENERGY.2015.12.073.

[4] T. Cholewa, A. Siuta-Olcha, and M. A. Skwarczyński, "Experimental evaluation of three heating systems commonly used in the residential sector," *Energy Build.*, vol. 43, no. 9, pp. 2140–2144, Sep. 2011, doi: 10.1016/J.ENBUILD.2011.04.026.

[5] S. Jacobs *et al.*, "Grouped Charging of Decentralised Storage to Efficiently Control Collective Heating Systems: Limitations and Opportunities," *Energies*, vol. 16, no. 8, 2023, doi: 10.3390/en16083435.

[6] S. Jacobs, F. Van Riet, and I. Verhaert, "A collective heat and cold distribution system with decentralised booster heat pumps: a sizing study," in *Building Simulation Conference Proceedings*, 2022, pp. 223–230, doi: 10.26868/25222708.2021.30423.

[7] L. Peeters, J. Van der Veken, H. Hens, L. Helsen, and W. D'haeseleer, "Control of heating systems in residential buildings: Current practice," *Energy Build.*, vol. 40, no. 8, pp. 1446–1455, Jan. 2008, doi: 10.1016/J.ENBUILD.2008.02.016.

[8] I. Verhaert, F. Van Riet, R. Baetens, M. De Pauw, and M. Van Erdeweghe, "Performance evaluation of different micro-CHP configurations in real life conditions and the influence of part load behaviour," *E3S Web Conf.*, vol. 111, p. 01084, Aug. 2019, doi:

10.1051/E3SCONF/201911101084.

[9] H. Averfalk, F. Ottermo, and S. Werner, “Pipe sizing for novel heat distribution technology,” *Energies*, vol. 12, no. 7, Apr. 2019, doi: 10.3390/en12071276.

[10] CEN, “EN 12828:2012+A1:2014 Heating systems in buildings - Design of water-based heating systems,” 2014.

[11] Z. Wang, J. Crawley, F. G. N. Li, and R. Lowe, “Sizing of district heating systems based on smart meter data: Quantifying the aggregated domestic energy demand and demand diversity in the UK,” *Energy*, vol. 193, Feb. 2020, doi: 10.1016/j.energy.2019.116780.

[12] T.-A. Koiv, A. Mikola, and U. Palmiste, “The new dimensioning method of the district heating network,” *Appl. Therm. Eng.*, vol. 71, no. 1, pp. 78–82, Oct. 2014, doi: 10.1016/J.APPLTHERMALENG.2014.05.087.

[13] I. Verhaert, “Design methodology for combined production and distribution for domestic hot water and space heating,” *E3S Web Conf.*, vol. 111, 2019, doi: 10.1051/e3sconf/201911101089.

[14] “VDI 2072: Heat transfer station with water/water heat exchangers for continueous-flow water heating/space heat,” Engl. VDI-Gesellschaft Bauen und Gebäudetechnik, 2019.

[15] K. Rühling *et al.*, “Energieeffizienz und Hygiene in der Trinkwasser-Installation" Kurzüberblick und Thesen FKZ 03ET1234 A bis D Seite 1 Energieeffizienz und Hygiene in der Trinkwasser-Installation,” 2018.

[16] I. Verhaert, B. Bleys, S. Binnemans, and E. Janssen, “A Methodology to Design Domestic Hot Water Production Systems Based on Tap Patterns,” *CLIMA2016 - Proc. 12th REHVA World Congr.*, 2016, [Online]. Available: http://www.wtcb.be/homepage/download.cfm?dtype=research&doc=paper_467.pdf&lang=en&lipi=urn%3Ali%3Apage%3Ad_flagship3_profile_view_base%3BiVwKZVBlRFaXZiH5ub6n4w%3D%3D.

[17] “VIS traject Instal2020: Integraal ontwerp van installaties voor sanitair en verwarming.” https://www.instal2020.be/.

[18] European Standard, “EN 12831-1:2017. Energy performance of buildings - Method for calculation of the design heat load - Part 1,” 2017.

[19] M. Noussan, M. Jarre, and A. Poggio, “Real operation data analysis on district heating load patterns,” *Energy*, vol. 129, pp. 70–78, Jun. 2017, doi: 10.1016/J.ENERGY.2017.04.079.

[20] T. Catalina, J. Virgone, and E. Blanco, “Development and validation of regression models to predict monthly heating demand for residential buildings,” *Energy Build.*, vol. 40, no. 10, pp. 1825–1832, Jan. 2008, doi: 10.1016/J.ENBUILD.2008.04.001.

[21] S. Hammarsten, “A critical appraisal of energy-signature models,” *Appl. Energy*, vol. 26, no. 2, pp. 97–110, Jan. 1987, doi: 10.1016/0306-2619(87)90012-2.

[22] L. Pedersen, J. Stang, and R. Ulseth, “Load prediction method for heat and electricity demand in buildings for the purpose of planning for mixed energy distribution systems,” *Energy Build.*, vol. 40, no. 7, pp. 1124–1134, Jan. 2008, doi: 10.1016/J.ENBUILD.2007.10.014.

[23] E. Guelpa, L. Marincioni, M. Capone, S. Deputato, and V. Verda, “Thermal load prediction in district heating systems,” *Energy*, vol. 176, pp. 693–703, Jun. 2019, doi: 10.1016/J.ENERGY.2019.04.021.

[24] S. Idowu, S. Saguna, C. Åhlund, and O. Schelén, “Applied machine learning: Forecasting heat load in district heating system,” *Energy Build.*, vol. 133, pp. 478–488, Dec. 2016, doi: 10.1016/J.ENBUILD.2016.09.068.

[25] D. Geysen, O. De Somer, C. Johansson, J. Brage, and D. Vanhoudt, “Operational thermal load forecasting in district heating networks using machine learning and expert advice,” *Energy Build.*, vol. 162, pp. 144–153, 2018, doi: 10.1016/j.enbuild.2017.12.042.

[26] E. Himpe and A. Janssens, “Data-Driven Modelling of the Energy Use in Dwellings using Smart Meter Data,” *CLIMA 2016 - Proc. 12th REHVA World Congr.*, 2016.

[27] H. Gadd and S. Werner, “Heat load patterns in district heating substations,” *Appl. Energy*, vol. 108, pp. 176–183, Aug. 2013, doi: 10.1016/J.APENERGY.2013.02.062.

[28] D. Ramon, K. Allacker, F. De Troyer, H. Wouters, and N. P. M. van Lipzig, “Future heating and cooling degree days for Belgium under a high-end climate change scenario,” *Energy Build.*, vol. 216, p. 109935, Jun. 2020, doi: 10.1016/j.enbuild.2020.109935.

[29] gas.be, “Graaddagen - Gas.” https://www.gas.be/nl/graaddagen (accessed Apr. 25, 2020).

[30] “K-peil | Vlaanderen.be.” https://www.vlaanderen.be/epb-pedia/epb-plichtig-toepassing-en-eisen/epb-eisen/k-peil (accessed May 11, 2020).

[31] “RMI - Automatic weather stations.” https://www.meteo.be/en/about-rmi/observation-network/automatische-weerstations (accessed Sep. 13, 2023).

[32] “Weerstation Kempen.” https://www.weerstationkempen.be/website2/ (accessed Sep. 13, 2023).

[33] “EN 1434-1:2015 Heat meters -Part 1: General requirements,” 2015.